

Neural networks for long term prediction of fouling and backwash efficiency in ultrafiltration for drinking water production

N. Delgrange-Vincent^a, C. Cabassud^{a*}, M. Cabassud^b,
L. Durand-Bourlier^c, J.M. Laine^c

^a*Laboratoire d'Ingénierie des Procédés de l'Environnement, INSA, 135 Avenue de Rangueil, 31077 Toulouse Cedex 4, France
Tel. +33 (5) 61 55 97 73; Fax +33 (5) 61 55 97 60; e-mail: cabassud@insa-tlse.fr*

^b*Laboratoire de Génie Chimique - UMR CNRS 5503, INPT/UPS, 18 chemin de la Loge, 31078 Toulouse Cedex 4, France
Tel. +33 (5) 62 25 23 62; Fax +33 (5) 62 25 23 18; e-mail: michel.cabassud@ensigct.fr*

^c*Centre International de Recherche sur l'Eau et l'Environnement, Lyonnaise des Eaux, Avenue du Président Wilson,
78230 Le Pecq, France*

Received 3 July 2000; accepted 17 July 2000

Abstract

The aim of this study was to develop a neural network model to predict the productivity of an ultrafiltration pilot plant, treating surface water to produce drinking water and operated with sequential backwashes. The model had to predict long-term performances of the pilot plant, it means to consider both reversible and irreversible fouling. The model had also to take into account a minimum number of parameters. On site experiments were performed to constitute the learning and validation databases. The developed model consists in two interconnected recurrent neural networks. It allows predicting satisfactorily the filtration performances of the experimental pilot plant for different resource water quality and changing operating conditions.

Keywords: Neural networks; Long-term modelling; Fouling; Ultrafiltration; Drinking water production

1. Introduction

Ultrafiltration by hollow fibre membranes is in increasing development in the field of drinking water production. It allows producing

drinking water from surface water, and to meet the requirements for water quality even in the case of resource degradation [1,2]. Nowadays, more than 50 UF plants for this application are in operation in the world. Most of the research activities in this field now focus on different ways to enhance plant's productivity. But

*Corresponding author.

advanced control strategies require models describing the influence of operating parameters, in order to perform short or long-term predictions of the plant behaviour.

Phenomena involved during filtration of surface water are very complex because of the nature of the fluid concerned. The first limiting phenomenon is particle deposition on the membrane surface, which appears at the scale of a filtration cycle (short-term); the procedure used to remove this particle cake deposit is the backwash performed with ultrafiltrated water. The second limiting phenomenon is adsorption of organic matter on the surface and into the membrane pores, which is a long-term phenomenon. The part of fouling which is removable by backwash is often called reversible fouling, the other part is called irreversible fouling.

Parameters that could be involved in fouling in the case of raw water treatment are numerous (water quality parameters and operating parameters) and interdependent. One possible way to know how to increase the plant productivity is to better understand phenomena involved in fouling and to develop a predictive model. Despite the great number of studies focusing on fouling, phenomenological models developed for ideal solutions are not applicable to describe membrane fouling by natural waters. As far as a large number of data could be obtained from pilot plants, statistical models appear as promising tools for developing simulation models. Among such tools, the model chosen in this work lies on artificial neural networks (ANNs).

In a previous study, ANNs were successfully used to predict short-term performances [3]. The aim of this study is to develop a model to predict the productivity of a plant from both water quality and operating parameters at a long-term scale, taking into account a minimum number of parameters. A preference will be given to water parameters that are easy and cheap to measure so as the model could be later set up on industrial plants for simulation or control.

2. Neural networks

ANNs can be developed to simulate any process by auto-organisation of their parameters during a learning phase. The parameters are optimised in order to model the functionality between the input and output vectors. Their design is realised by learning (or optimisation) from a set of numerical values (the learning data base). This general character, together with their properties of non-linearity and massive parallelism, enables their use in many applications where numerous and noisy data occur. In chemical engineering, ANNs have so far mainly been used in process modelling, process control, fault diagnosis, error detection, data reconciliation and process analysis [4–8].

An example of network structure is introduced in Fig. 1. The input layer of the network does not perform any treatment but acts as a mean by which scaled data are introduced to the network. The data from the input neurones are propagated through the network via interconnections. Every neurone in a layer is connected to every neurone in adjacent layers. A scalar weight is associated with each interconnection. The neurones within the hidden layers perform two tasks: they sum the weighted inputs to the neurone and, then, pass the resulting summation through a non-linear activation function. A bias term is associated with each interconnection in order to shift the space of the non-linearity.

The topology of any ANN determines the accuracy and the domain of representation of the model. Many papers have shown that a feed forward network has the potential to approximate any non-linear function. In this paper, a single hidden layer has been considered, as the universal approximation theory [9] suggests that a network with a single hidden layer can link inputs and outputs with a good accuracy if the number of neurones in the hidden layer is sufficient. The number of neurones in this hidden

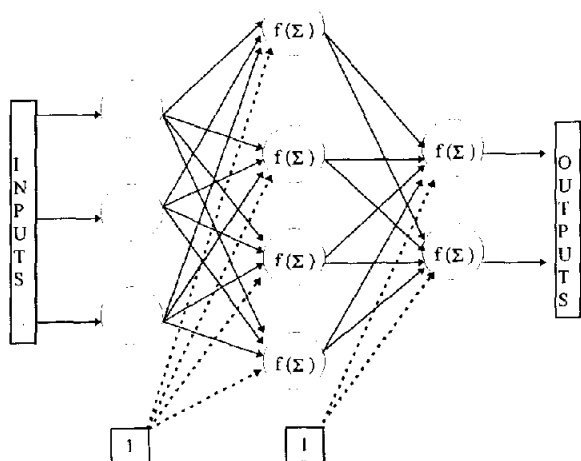


Fig. 1. Architecture of a neural network with 3 input neurones, 1 hidden layer with 4 neurones, and 2 output neurones.

layer has been chosen by a trial and error procedure.

One important aspect in an ANN development procedure is the learning process. Representative examples are presented to the network so that it can integrate the corresponding knowledge within its structure. The learning process consists in determining the weights $w_{j,i,k}$ that produce the best fit between the actual and the predicted outputs over the entire training region. The weights are first set to random values. An input vector is then impressed on the input layer and is propagated through the network to the output layer.

The difference between the computed outputs (O_3) and the target vector (T) is used to determine the weights using an optimisation technique in order to minimise the sum of the squares of the errors (F). The errors between networks outputs and targets are summed over the entire data set and updating of the weights is performed after every presentation of the complete data set.

Theoretical and numerical results proved that quasi-Newton algorithms are superior to steepest algorithms. Watrous [10] employed and compared DFP and BFGS methods with the back-propagation algorithm: this comparison showed that DFP and BFGS need fewer iterations. For this reason, a quasi-Newton [11] learning algorithm has been used to train the neural nets.

Two data sets are considered for the learning phase. The first one, called the learning data set, is used to calculate F and to update the weights. The second one, called the test data base, is used to determine the optimal weights which give the minimum error on this test base.

The first step in the study is data collection which has to be performed with a specific attention concerning the choice of the parameters to be measured and the measurement method.

3. The pilot plant and data collection

The pilot plant schematised in Fig. 2 used one module of cellulose acetate hollow fibres, inner diameter 0.93 mm. The module filtering area S was 7.2 m². Raw water was pre-filtered to 200 μm, then injected in the circulation loop by the feed pump P1.

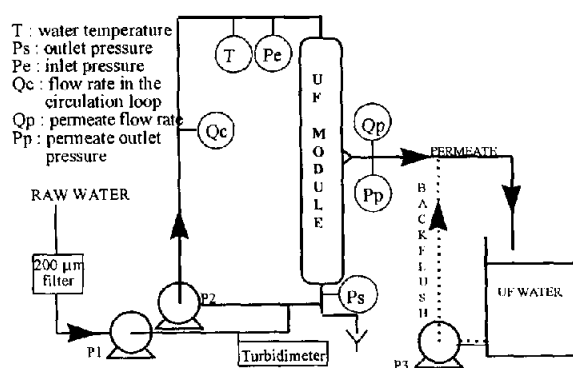


Fig. 2. The UF pilot plant.

The pilot produced a constant permeate flow rate (Q_p), leading to a pressure increase during the filtration time. The feed velocity at the module inlet was fixed by the circulation flow rate (Q_c). Sequential backwashes were automatically operated with a constant volume of chlorinated permeated water. They allowed to decrease the pressure and to restart a new filtration cycle. The total hydraulic resistance R is defined by

$$R = T_{mp} / (\mu \cdot Q_p / S) \quad (1)$$

where μ is the water viscosity which is temperature dependant, and T_{mp} is the mean transmembrane pressure. The total resistance R includes the membrane resistance, the resistance due to reversible fouling and the resistance due to irreversible fouling. In the case of a constant permeate flow rate, the resistance increases during the filtration period and decreases after backwash, as presented in Fig. 3. Therefore a production curve is composed of cycles, each characterised by the resistance at the end of the filtration cycle ($R-e$) and at the beginning of the next cycle, i.e. after backwash ($R-b$). Time variations of $R-b$ and $R-e$ are then sufficient to characterise and to describe the filtration process variations.

Data were collected during experiments carried out with surface water during a long test period. Transmembrane pressures at the beginning and at the end of the cycle are recorded continuously as well as different parameters:

- concerning water quality : turbidity (TUR), pH, dissolved oxygen (O_2), UV absorbency, Total Organic Carbon (TOC), temperature (T), oxido-reduction potential (Eh)
- concerning both filtration and backwash operating conditions: permeate flow rate (Q_p), circulation flow rate (Q_c), filtration time (t_f), chlorine concentration in the backwash water

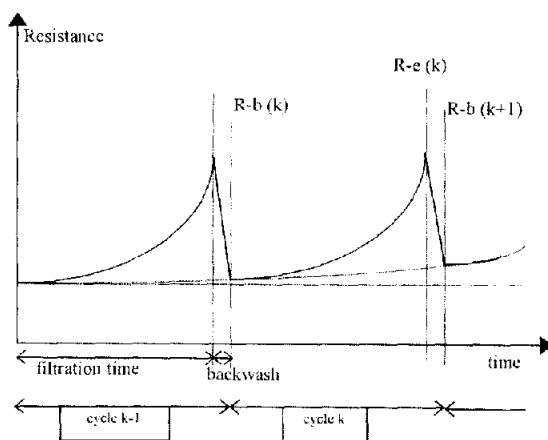


Fig. 3. Example of resistance time-variation.

($[Cl]_{RL}$), backwash pressure (P_{RL}), backwash duration (t_{RL}).

The range of these parameters is introduced in Table 1.

The whole data base was composed of 12 curves, each containing between 60 and 140 filtration/backwash cycles. It totalled about 1050 cycles.

An example of experimental result is shown in Fig. 4. During the experiment shown on this figure the water parameters varied with time, as a natural river water was used. Most of the operating parameters were maintained constant. The only process parameter which was varied was the permeate flux (Fig. 4a). At a low permeate flux (40 l.h.m^{-2} at 20°C) T_{mp} and resistance at cycle start and at cycle end were nearly equal and were constant over 11 cycles which means that both reversible and irreversible fouling were negligible (Figs. 4b and 4c). Then the permeate flux was increased to 60 l.h.m^{-2} for a period of 30 cycles. A step in T_{mp} is then immediately observed, as expected according to Darcy's law. T_{mp} at cycle end was then higher than T_{mp} at cycle start and both increased slowly with time. Reversible and irreversible fouling began to appear. The permeate flux was then increased

Table 1

Range of water quality parameters and of operating parameters

	TUR, NTU	pH	O ₂ , mg/l	UV, m ⁻¹	TOC, mg/l	T, °C	Eh, mV	Qp/S, l.h ⁻¹ .m ⁻²	Qc, m ³ /h	tF, min	[Cl] _{RL} , mg/l	P _{RL} , bar
min	0.25	7.4	4	1.5	0.5	5	150	40	=Qp	20	2	1.5
max	170	8.5	9	11	5.5	16	950	100	6	60	20	2.5

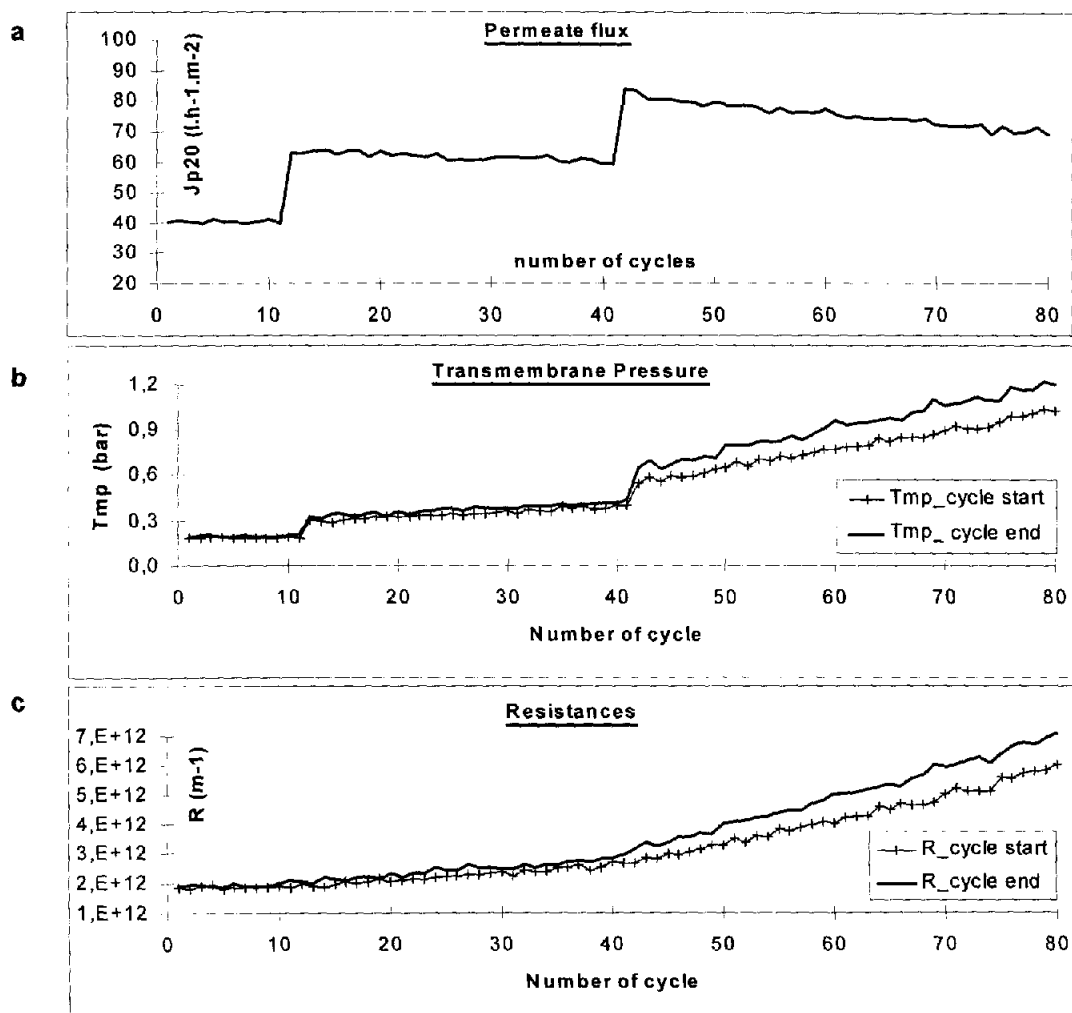


Fig. 4. Example of experimental results on the influence of the permeate flux on transmembrane pressure and on total resistance for a surface water: a, imposed values of the permeate flux at 20°C vs. the number of cycle; b, variation of Tmp at cycle start and at cycle end; c, variation of total resistance.

to a value between 70 and 80 l.h.m⁻² which induced an increase of both fouling phenomena.

4. Long-term modelling

In the field of process engineering, neural networks have successfully been used in process modelling and control [4–8], and some trials have been promising in the field of crossflow microfiltration of cane sugar [12] and of baker's yeast [13], reverse osmosis of ethanol and acetic acid [14] and ultrafiltration of surface water [3], of bleach plant effluents [14] and of proteins [15]. Niemi et al. [14] computed UF and reverse osmosis permeate flux and rejections by ANNs and ANNs predictions were compared with results from a phenomenological model. ANNs was found easier to use, more efficient and sufficiently accurate for industrial design.

In a previous study, neural networks have been successfully used to predict short-term performances for UF for drinking water production [3]: pressure at the end of a filtration cycle and at the beginning of the next cycle (i.e. after backwash) can be calculated using one water parameter (turbidity) and some operating parameters at the cycle-beginning. At a cycle scale, the most important effect is reversible fouling, due to cake deposition. This is the reason why a one step prediction neural network using only turbidity was able to predict the evolution of resistance.

In this paper the objective is to develop a long term predictive model, it means to be able to compute resistances at cycle ends and at cycle starts on a long term, just knowing the time variation of water quality parameters and of operating parameters that can vary from one cycle to the other. The only resistance data given to the model is the one measured at time 0. The model thus requires a recurrent neural network. Moreover, it is necessary to take into account the

evolution of the irreversible part of fouling, which is not removed by backwashes. It necessitates to incorporate some other water quality parameters as neural network inlets, and to consider the backwash operating parameters. For example, Figs. 7 and 8 which present some experimental results are characteristic of two different behaviours. In the first case, backwashes are efficient to remove fouling, as the Tmp at cycle starts remains quite constant during the whole experiment. In the second case, described in Fig. 4 too, the resistance gradually increases, which means that irreversible fouling occurs, backwashes are not efficient enough to remove fouling in this case.

4.1. Model architecture

Different neural networks have been developed. The best model consists of two interconnected neural networks. The first one is specialised in the prediction of the resistance at the cycle end while the second computes the resistance at the next cycle beginning (i.e. after backwash). In the first network, the inlets should be the resistance at the current cycle beginning, and water quality parameters that are necessary to quantify fouling. In the second one, the inlets should be the resistance at the end of the filtration period, the water quality parameters previously used to quantify fouling, and the operating conditions during the backwash procedure to predict the backwash efficiency. These considerations lead to the architecture presented in Fig. 5.

4.2. Neural network architecture and training

The neural networks used in this modelling are composed of three layers: an input layer, one hidden layer and an output layer. Every neurone

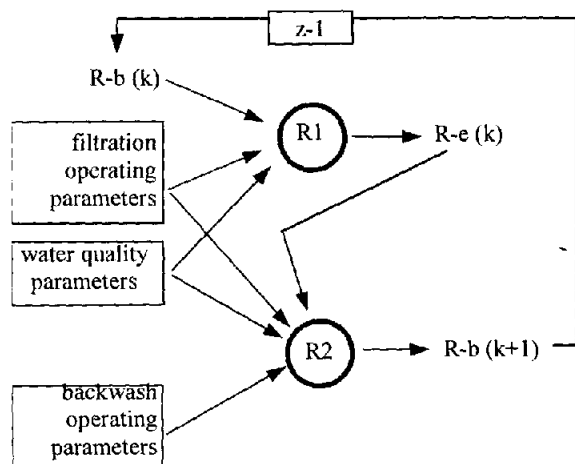


Fig. 5. Schema of the interconnected neural networks.

in a layer is connected to each one in adjacent layers. A scalar weight is associated with each interconnection. A bias neurone is introduced in the input and hidden layers. The activation function used is the sigmoidal function f defined by :

$$f(x) = \frac{1}{1 + \exp(-x)} \quad (2)$$

The whole data base is divided into three sets: the training set is composed of about 400 cycles, the test set is composed of about 200 other cycles, and all the points compose the generalisation set. The neural networks are independently trained using a non-recurrent procedure, then connected and used recurrently.

The weights are first set to random values. The input vectors are then submitted to the network, and the weights are optimised in order to minimise the error F , defined by the summation on the entire training set of the squares of the errors:

$$F = \frac{1}{2} \sum_{k=1}^{N_t} [T(k) - O(k)]^2 \quad (3)$$

where N_t is the number of example points (i.e. cycles) in the training set, $T(k)$ is the targeted output for cycle k and O is the computed output for cycle k . The optimisation technique used in this study is a quasi-Newton algorithm [11]. The weights leading to the minimum error on the test data base are the optimal weights. The test set is then used to determine the iteration which leads to the optimal weights.

A neural network structure is tested on several initial random weight sets, for different numbers of neurones into the hidden layer.

5. Results

Different neural network models were built, varying the parameters taken as network inlets to find the significant ones. The parameters found to be the more significant are the permeate flow rate, the filtration time, turbidity, dissolved oxygen, pH, UV, backwash pressure and chlorine concentration.

The only resistance data given to the network R1 is the one at time 0. The parameters concerning water quality that have been shown to be sufficient are turbidity, dissolved oxygen, pH and UV absorbency. It means that TOC and the oxido-reduction potential are not necessary to describe membrane fouling by this specific surface water. First trials were made including these two parameters on the considered database but compared to the present results, they did not significantly increase the prediction accuracy. This is an interesting result, because TOC is a parameter which is difficult and expensive to measure on line, and the oxido-reduction electrode has a quite high time constant. Their influence on fouling is probably not negligible, but it is certainly taken into account by the other

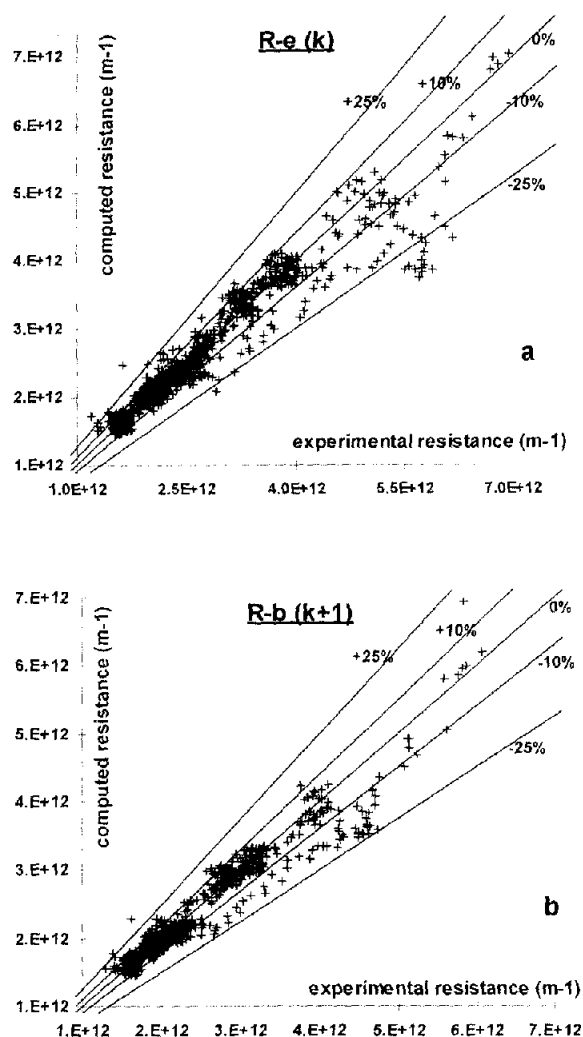


Fig. 6. Computed resistance vs. experimental resistance: a, at the cycle end $R-e(k)$; b, after backwash $R-b(k+1)$.

water quality parameters combination. Easy and cheap to measure parameters are preferable, so as the model could be later set up on industrial plants for simulation and control.

The results on the generalisation data base, i.e. on all the available points, are summarised in Fig. 6, representing the computed resistances vs. the experimental resistances.

90% of the computed values fit the experimental ones with an error less than 10%. Only 1% of them reach an error over 25%, these points concerning a part of the same curve. For the smallest resistance values, the low measurement accuracy leads to a high uncertainty (about 100%) for the resistance. It causes some computed resistance values exceeding an error of 10%.

When no irreversible fouling occurs, the resistance at cycle starts remains constant: fouling is reduced to a cake deposit. However when adsorption phenomena occur, the resistance slowly increases, backwashes are not efficient enough to clean the membrane. This low resistance increase is not easy to model, because of the physical phenomena complexity.

The majority of resistance values are computed with a satisfying accuracy (less than 25%), with a long-term prediction. Using Eq. (1), the results can be explained using transmembrane pressures instead of resistances.

The sample curve 1 in Fig. 7 contains about 140 cycles. During the experiments, almost all the measured parameters (concerning water quality and operating conditions) varied. The permeate flux, the filtration time and backwash chlorine concentration were varied, and during the experiment almost all the parameters concerning water quality changed in a large scale (turbidity from 5 to 120 NTU, O_2 from 8.5 to 4.5 $mg.l^{-1}$, TOC and UV increased respectively from 3 to 4.5 $mg.l^{-1}$ and from 4.5 to 8 m^{-1}). In Fig. 7, the lines represent the experimental time evolution of the transmembrane pressure at cycle end (continuous line) and at next cycle beginning (continuous line with dashes). Corresponding computed pressures are represented respectively by circles and by lozenges. We can notice that the computed values fluctuate, but they are quite stable, compared to the experimental ones (no parameter in inlet is smoothed). The shape is respected for the 12 curves, even for long time predictions (over 80 cycles).

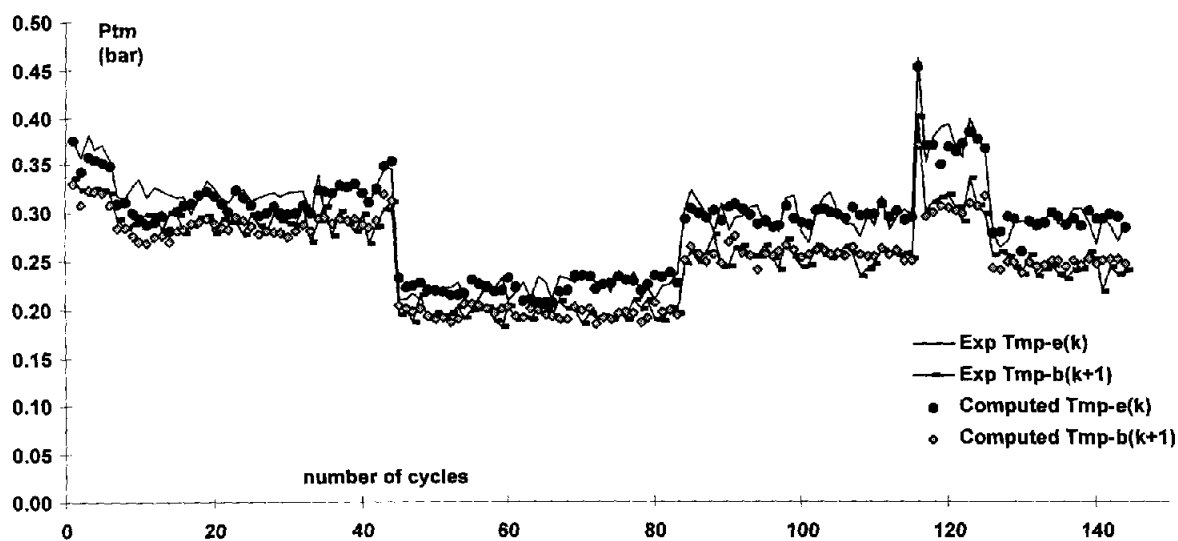


Fig. 7. Sample curve 1.

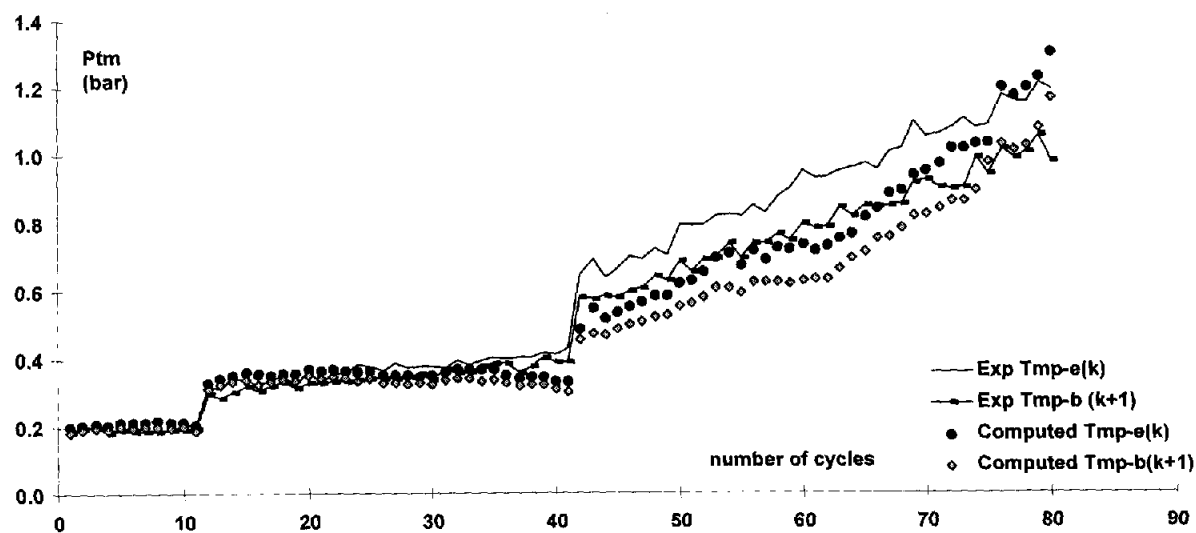


Fig. 8. Sample curve 2.

The sample curve 2 (Fig. 8) is related to irreversible fouling, as the pressure increases gradually. The three steps correspond to three different permeate fluxes (see Fig. 4). On this experiment, the resistance increases gradually.

Even in this case, the shape of the resistance evolution is correctly predicted, and the computed values fit the experimental ones with a satisfying accuracy (less than 25%). Moreover, the distance between computed and experimental curves tends to reduce.

6. Conclusion

A neural network model was built to predict the evolution of resistance, or transmembrane pressure, in the case of surface water treatment by an ultrafiltration module. This recurrent model allows a good prediction, even in the case of changing water quality, at a long-term scale (more than 100 filtration cycles, i.e. several days of operation). It combines two neural networks, independently trained, then connected and used recurrently. The aim is now to introduce this neural network model into the control strategy of the pilot plant.

References

- [1] C. Cabassud, C. Anselme, J.L. Bersillon and P. Aptel, *Filtration & Separation*, 28 (1991) 194.
- [2] C. Anselme and E.P. Jacobs, *Ultrafiltration*, Ch.10 in: *Water Treatment Membrane Processes*, McGraw-Hill, 1996.
- [3] N. Delgrange, C. Cabassud, M. Cabassud, L. Durand-Bourlier and J.M. Laine, *J. Membr. Sci.*, 150 (1998) 111.
- [4] A.J. Morris, G.A. Montague and M.J. Willis, *Trans. IChemE.*, 72 (1994) 3.
- [5] J.L. Dirion, B. Ettegui, M. Cabassud, M.V. Le Lann and G. Casamatta, *Chem. Engng. and Processing*, 35 (1996) 225.
- [6] A.B. Bulsari, *Neural Networks for Chemical Engineers*. Elsevier, Amsterdam, 1995.
- [7] Sege G. and Woodfield F.W., *Chem. Eng. Progr.*, 50 (8)(1954) 396.
- [8] A. Chouai, M. Cabassud, M.V. Le Lann, C. Gourdon and G. Casamatta, *Chem. Engng. and Proc.*, 39 (2000) 171.
- [9] S.S. Tambe, B.D. Kulkarni and P.B. Deshpande, *Elements of Artificial Neural Networks with selected Applications in Chemical Engineering and Chemical and Biological Sciences*, Simulation and Advanced Controls Ltd., Louisville, KY, USA, 1996.
- [10] R.L. Watrous, *Proc. of IEEE First Int. Conf. Neural Networks*, (1987) pp. 619-627.
- [11] J.E. Dennis and R.B. Schnabel, *Numerical Methods for Unconstrained Optimisation and Non-linear Equations*. Prentice-Hall, New Jersey, 1983.
- [12] M. Dornier, M. Decloux, G. Trystram and A. Lebert, *J. Membr. Sci.*, 98 (1995) 263.
- [13] E. Piron, E. Latrille and F. René, *Comp. Chem. Engng.*, 21 (1997) 1021.
- [14] H. Niemi, A. Bulsari and S. Paloraasi, *J. Membr. Sci.*, 102 (1995) 185.
- [15] W.R. Bowen, M.G. Jones and H.N.S. Yousef, *J. Membr. Sci.*, 146 (1998) 225.